Synthesis of silk sericin stabilized silver (Ag-Ser) nanoparticles using Tollens' method and investigation of its colloidal stability

Mert Saraçoğlu (saracoglum16@itu.edu.tr)
Istanbul Teknik Üniversitesi: Istanbul Teknik Universitesi https://orcid.org/0000-0001-8036-0396
Begüm Bacınoğlu
Università degli Studi di Milano Dipartimento di Scienze e Tecnologie Biomediche: Universita degli Studi di Milano Facolta di Medicina e Chirurgia
Sıddıka Mertdinç
Istanbul Technical University: Istanbul Teknik Universitesi
Servet Timur
Istanbul Teknik Universitesi - Ayazaga Kampusu: Istanbul Teknik Universitesi

Research Article

Keywords: Silver nanoparticles, Surface functionalization, Sericin, Tollens' method, Colloidal stability

Posted Date: December 13th, 2021

DOI: https://doi.org/10.21203/rs.3.rs-1141192/v1

Abstract

In this study, sericin extracted from *Bombyx mori* silk cocoons was integrated into the well-known Tollens' method for synthesizing Ag-NPs. Sericin successfully acted as a stabilizer while silver amine complex $[Ag(NH_3)_2]^+$ was reduced by maltose. As a result, silver nanoparticles with high stability are formed. Possible functional groups related to the stabilization of NPs were investigated by Fourier-transforms infrared spectroscopy (FT-IR). Ag-Ser NPs were characterized by using particle size measurements based on dynamic light scattering (DLS) and transmission electron microscopy (TEM). According to the characterization investigations, Ag-Ser NPs have characteristic (111) face-centered cubic (FFC) plane and were spherical in shape with a narrow size distribution of 20.23 ±6.25 nm. Overall, the sericin-modified Tollens' method for synthesizing Ag-NPs offers a simple and non-toxic production method to form nanoparticles. Colloidal stability of nanoparticles displays an essential role since their enhanced nano-properties can be diminished by an increase in size due to aggregation and agglomeration. Therefore, the effect of pH on particle stability was investigated through the surface charge of Ag-Ser NPs that was measured using a Zeta-potential analyzer. Results obtained from this study may extend the applicability of silver nanoparticles in biotechnological researches and a potential synthesis route for the application of Ag-Ser NPs as aseptic and therapeutic usages.

1. Introduction

Materials with at least one dimension in nanometer scale such as; nanofibers, nanocapsules, nanorods, nanotubes, and nanostructured surfaces are considered as nano-materials. Thus, synthesizing, manipulating and controlling the nanometer scale materials are the main interest of Nanotechnology [1], [2]. Nanomaterials other than their bulk forms, show superior mechanical, electrical, chemical, optical, magnetic, thermal, or biological properties due to their high surface area [2], [3]. Among them, silver based nanoparticles considered the most efficient and researched nanomaterials due to their broad biocidal effect [4]. Dissolution of Ag^0 to Ag^{+1} gives rise to the random formation of silver complexes hence inhibiting the responsible proteins for RNA-DNA replication and increase the permeability of the membrane [5]. Consequently, it shows outstanding antifungal, antibacterial and antiviral properties [6]. Therefore, silver nanoparticles are extensively used in various biomedical applications including wound dressings, disinfectants and catheters [7]–[9].

Chemical reduction of silver ions is the most commonly used nanoparticle production method due to simplicity and being cheaper than the physical and mechanical production techniques.[12] However, using reductants and stabilizers in reduction protocols can be highly toxic for both environment and human health [10], [11]. Hence, usage of these chemicals results in problems by hindering their further usage in biomedical applications such as drug delivery, antibacterial agent [12]. To avoid such complications, green synthesis of nanoparticles is required.

Furthermore, the usage of silver NPs is limited due to their instability against aggregation. Consequently, antimicrobial and catalytic activities are diminished by the aggregates that reduce the surface area of

particles [13]. To benefit from enhanced properties of silver NPs, particles acquired to be stabilized. Stabilization occurs mainly by two mechanisms: electrostatic repulsion by charged molecules and steric repulsion by adsorption of complex polymers on the particle surface [14]. For this reason, complex biopolymers with ability to stabilize in both mechanisms, show an excellent opportunity for green, large-scale silver nanoparticle production. In literature, natural polymers such as polysaccharides, chitosan, and gelatin have proven to stabilize nanoparticles and natural reductants, such as ascorbic acid and sugars, successfully reduce silver ion [15]–[19].

Sericin is also a bio-complex polymer that constitutes 20% - 30% of silk cocoon and preserves structure unity [20]. Over the years, the interest in sericin protein in bio-nanotechnology has been increased due to its biomedical applications owing to have distinctive properties such as UV-protection, anti-oxidative ability and bio-compatibility [13], [21]. Sericin is selected as a stabilizing agent due to its electrostatic and steric protection, owing to its long molecular structure and high hydrophobicity [13]. Consequently, aggregation and degradation of particles can be prevented.

In this study, we have extracted and used sericin from silk cocoons to synthesize sericin-coated silver nanoparticles (Ag-Ser NPs) based on the Tollens process. Traditional Tollens process was used for mirror making by electroless deposit silver particles on a surface [22]. Formerly, it has been proven that colloidal silver nanoparticles can be synthesized by the Tollens process based on pH, the concentration of reaction components, and stabilizer media [23]. Process parameters were optimized according to average particle size of Ag-Ser NPs. To investigate the role of sericin in nanoparticle stabilization, Ag-Ser NP's stability was measured at various pH values to simulate biologically relevant conditions to enable the integration of NPs in biomedical uses.

Herein, the usage of sericin individually as a stabilizer in silver nanoparticle synthesis, providing both electrostatic and steric stabilization for nanoparticles at a wide pH range. Thus, synthesis of stable Ag-Ser NPs with a low cost, non-toxic route could allow future usage of silver nanoparticles in biomedical applications.

2. Experimental Section

2.1. Materials. *Bombyx Mori* silk cocoons were obtained from Kozabirlik (Bursa, Turkey) as a sericin source. Silver nitrate ($AgNO_3$, Merck^{TM}, 99.99%), ammonium hydroxide (NH_4OH, Merck^{TM}, %25 w/w), sodium hydroxide (NaOH, Merck^{TM}), D-(+)-maltose monohydrate (Merck^{TM}) were used as initial materials. Bovine Serum Albumin (BSA, Sigma-Aldrich^{TM}) and Bradford reagent (Bio Basic^{TM}) were used in experiments as raw materials. Distilled water were used in all steps of the experimental procedures. All glassware equipment was immersed in 30% nitric acid (v/v) and rinsed with deionized water prior to use.

2.2. Sericin extraction. Initially, *Bombyx Mori* silk cocoons were cut into smaller pieces. Then, freshly sheared 4.5 g cocoon into 300 mL distilled water was autoclaved under the 1 atm pressure at 121 °C for 1

hour. After that, Sericin solution was vacuum filtered through 2 µm filtering paper to remove any impurities [24].

2.3. Protein quantification analysis by Bradford Assay. 1 mL of BSA solutions were prepared in various concentrations of 0.0, 0.125, 0.25, 0.5, 0.75, 1.0 and 1.25 (mg/mL). Each cuvette contained 1200 µL of Bradford Reagent and 20 µL of the protein samples. 3 cuvettes for each concentration were measured and the mean absorbance values were taken. Every cuvette was incubated 5 minutes before measuring at 595 nm. After quantifying all of the BSA solutions, the isolated sericin samples were measured. Then, according to the mean values of each result, the protein quantity was estimated with R^2=99.

2.4. Synthesis of silver nanoparticles via modified Tollens Method. For synthesis, the modified Tollens method was employed by addition of sericin as a stabilizer [14]. Briefly, 1 mM $AgNO_3$ solution was mixed with 5 mM, 10 mM and 15 mM NaOH (Based on pH) to obtain Ag_2O. Then the stoichiometric amount of NH_4OH was added to the mixture to obtain silver amine complex ($[Ag(NH_3)_2]^+$). Extracted sericin solutions were added into the mixture containing silver amine complex, with concentration ranging from 10 to 25 µg/mL. Finally, 20mM maltose monohydrate was added to the mixture as a reducing agent. Reaction components were added to the mixture in the mentioned order with vigorous stirring. Followed by synthesis, Ag-Ser NPs were stored at +4 ºC under light-sensitive conditions to avoid further agglomeration of particles.

2.5. ATR-FTIR Spectroscopy analysis. FTIR spectra of the specimens were recorded at room temperature in the mid-IR range (400 – 4000 cm^{-1}) on a Bruker Alpha-p FTIR spectrometer equipped with a Bruker Platinum ATR accessory. Sample measurements were conducted on dry, lyophilized sericin powder. Each spectrum was taken over 12 scans with a resolution of 1 cm^{-1}. Obtained results were analyzed using OPUS Software (Bruker Optics). For all experiments, Ag-Ser NPs synthesized with 1mM $AgNO_3$ and 25 µg/mL sericin at pH of 11.5 were used.

2.6. Nanoparticle Characterization. The mean particle size of Ag-Ser NPs was recorded using particle size analyzer NanoFlex™ particle measurement device, based on the dynamic light scattering (DLS). All experiments were repeated three times prior to measurement. JEOL JEM 2100 transmission electron microscope (TEM) operating at 200kV, was used for morphological analysis of the synthesized Ag-Ser nanoparticles. Nanoparticle diameters were calculated using ImageJ processing and analysis software (version v1.52a) by measuring 100 diameters of the particle from 3 different TEM images at 15.000x

magnification. Additionally, selected area diffraction patterns (SADP) were taken from TEM images to help the phase identification of the silver nanoparticles.

3. Results And Discussion

3.1. Extraction and analysis of sericin protein. Sericin was extracted from silk cocoons for further usage in Ag-Ser NP synthesis. Sericin protein can be extracted by heat, acids, and bases. The biological and physical properties of sericin can be affected by different extraction method[24]. In this work, sericin has extracted by autoclaving for 60 min at 0.1 MPa with a degumming rate of %18-25 of total cocoon mass. This process is selected among others due to its simplicity and not contain any further purification steps [25].

Sericin molecules show characteristic amide (I-II-III) peaks in the IR spectrum. Amide I peak generally corresponds 1630-1650 cm^{-1} due to C=O stretching vibration whereas, N-H bending and C-N stretching vibration at 1520-1540 cm^{-1} for amide II and C-N stretching vibration together with N-H in-plane bending at 1270-1230 cm^{-1} for amide III [20], [26]. From FTIR measurements, (Figure 1.) amide (I-II-III) peaks were detected at 1652.8, 1530.7, and 1249.4 cm^{-1} respectively. It is worth to mention that the amide I and amide II presents the major peaks in the spectra corresponding to C=O stretching. Thus, relative intensity of C=O peaks indicates extracted sericin structure abundantly contains highly hydrophilic carboxylate groups.[20] Moreover, absorptions at 1050 and 1391 cm^{-1} arise from C-H and O-H bending vibration and C-OH stretching vibration also indicates structure rich in hydroxyl chains [26].

Furthermore, Amide bonds are the backbone of polypeptide chains thus, their absorptions in IR spectra could indicate molecular conformations and secondary structures of the proteins [26]. In a previous study, random coil structures were assigned to 1650 cm^{-1} for amide I, 1540 cm^{-1} for amide II and 1230 cm^{-1} for amide III [20]. As mentioned before, peaks that found at 1652.8, 1530.7 and 1249.4 cm^{-1} may show, sericin protein consist of a high degree of random coils [27]. This molecular conformation may suggest that the sericin molecules have denatured and degraded due to high temperature-high pressure extraction method. Thus, abundance of highly electronegative functional groups appeared on IR spectra, may produce an electrostatic barrier while, complex polymer structure provides a physical barrier to particle aggregation. Therefore, denatured sericin may be a promising stabilizing agent for nanoparticle synthesis.

3.2. (Ag-Ser) nanoparticle preparation and evaluation of synthesis parameters. Silver nanoparticle synthesis by Tollens process involves three reactions; formation of silver oxide by dissolution of $AgNO_3$ with presence of NaOH (Eq. 1), alteration of silver oxide to silver amine complex (Eq. 2) and reduction of silver amine complex cation in alkaline media by a reducing sugar (in this case maltose) (Eq. 3).

$2AgNO_3 + 2NaOH \rightarrow Ag_2O + 2NaNO_3 + H_2O$ (Eq. 1)

$Ag_2O + 4NH_4OH \rightarrow 2[Ag(NH_3)_2]^+ + 3H_2O$ (Eq. 2)

$R\text{-}CHO + 2[Ag(NH_3)_2]^+ \rightarrow 2Ag + 4NH_3 + 2H_2O + R\text{-}COONa$ (Eq. 3)

In nanoparticle synthesis, size distribution, morphology and stability are dependent on concentration of reaction components, type of reducing and stabilizing agents [28]. During the reduction of silver complex, ammonium concentration was remain same in all experiments since, excess NH_3 ions in solution surround the amine complexes thus, fewer silver nuclei can be formed due to slower reaction kinetics. Consequently, the particle size prone to be larger [29].

Table 1
Average particle sizes of synthesized Ag-Ser NPs at different pH conditions.

pH[a]	**11.5**	**11.8**	**12**
Average particle size[b] (nm)	20.23 ±6.25	38.7 ±14.5	51.8 ±23.01
[a] pH of solutions was measured before addition of maltose solution.			
[b] Concentration of sericin was kept same in all pH experiments (20µg/mL).			

In addition to ammonium concentration, pH value of the solution is also a crucial parameter for the Tollens process. As the pH of the reaction environment increased above 12, thick silver layer forms on the glass surface. (see appendix.) Consequently, particle production yield decreases. This phenomenon was also reported by S. Sangsuk [30]. In their work, sonication was applied in reaction system to avoid mirror formation. On the other hand, at pH values lower than 11.5 prolong reaction time from minutes to hours. Therefore, optimum pH values were determined between 11.5 and 12.

Particle size measurement results (Table 1.) show that size distribution of Ag-Ser NPs was increased from 20.23 ±6.25 nm to 51.8 ±23.01 nm from pH 11.5 to pH 12. Results are consistent with a previous studies, in which at pH of 11.5, both mean particle size and distribution become narrower [29]. Remarkably, adjusting pH of synthesis media to 11.5, provide both smaller average particle size and narrower standard deviation.

Table 2
Reaction time and particle distribution on different sericin concentrations

Sericin conc. (µg/ml)	**10**	**15**	**20**	**25**
Average particle size[a] (nm)	30.86 ±7.8 nm	28.9 ±7.41 nm	20.23 ±6.25 nm	18.04 ±6.03 nm
[a]pH of the solution were kept at 11.5 for all experiments.				

As for the sericin concentration (Table 2.), The lowest particle size value (18.04 ±6.03) were enabled via 25 µg/mL sericin concentration. Results suggest that reaction time can be affected by stabilizer concentration together with pH of the solution. Moreover, controlling both parameters has a crucial role in

synthesizing nanoparticles with optimum anti-bacterial activity since silver nanoparticles' anti-bacterial efficiency depends on their size [31].

3.3. TEM Results and estimation of sericin coating on Ag-Ser NPs. According to our TEM results (Figure 2.A-B), Ag-Ser NPs were consisted spherical particles with no indication of aggregation. Each equiaxed spherical shaped particles have nearly same diameters. Due to mono peak size distribution between 14 nm to 19 nm, the ripening process cannot be observable from particle distribution (Figure 2.D). However, on a single nanoparticle (Figure 2.B) grain boundaries are present in a multigrain structure. Therefore, results may direct the coalescence of first formed particles by the ripening process after the nucleation stage [32]. HRTEM image (Figure 2.C) presents Ag-Ser NPs have periodic lattice spacing of 0.23 nm, which consistent with the characteristic plane of (111) for face-centered cubic (FCC) structure [32], [33].

SAED patterns (Figure 3A,B) present a ring and spot diffraction pattern which also indicates polycrystalline nature of Ag-Ser NPs [34]. However, we detected some highly crystalline particles which further prove the ripening of particles at the growth stage. Interplanar distances ($d_{calculated}$) of patterns were found to be 2.33, 1.95, 1.37, 1.08, 0.85 and 1.04 Å which corresponds to (111), (200), (220), (222), (422) and (400) planes of face centered cubic structure (FCC) which is specific for Ag crystal structure [35], [36].

To investigate that the extracted sericin can encapsulate synthesized particles and stabilize the growth stage, both particle size measurements and TEM analyses were used. It is worth to mention that DLS measures particle diameters through fluctuations in light intensity [4]. Hence, recorded particle diameters with DLS also contain sericin coating, but TEM only provides particle images without the organic component due to the proteins' electron transparency. Consequently, the thickness of the sericin coating equals the difference between the two diameters. From TEM images of Ag-Ser particles, the mean particle diameter calculated from the size distribution histogram (Figure 2.D) is 16.03 ±2.3 nm. On the other hand, as shown in (Table 2.) size distribution, determined by particle size measurements analysis, was found to be 18.04 ±6.03 nm at same sericin concentration. In conclusion, the particle diameter difference between measurements indicates sericin successfully coated nanoparticle surface.

3.4. Zeta potential measurements of Ag-Ser nanoparticles. Zeta potential is a quantitative parameter, which shows the charge difference between the nanoparticle surface and the surrounding medium [4]. When the surface charge of particles is strong enough, Brownian diffusion processes will be the dominant force in the system and overcome attraction forces (in this case, Van der Waals forces) [37]. Therefore, evaluating the surface potential could be a useful tool to understand the electrostatic stability of Ag-Ser NPs.

When synthesized nanoparticles have considerable positive or negative zeta potential value (> ±30 mV), repulsion forces between particles are supposed to be high. Thus, particles will not intent to be agglomerated [38]. In the nanoparticle–sericin system, charge difference emerges from negative –oxo, -

hydroxo, sulfide, and carbonyl groups from sericin coating or free OH^- ions in the solution environment [37]. Therefore, a decrease in pH can reduce the electrostatic stability of nanoparticles.

Table 3
Zeta potential values of Ag-Ser NPs at different pHs varied from 4.5 to 10.

pH	4.5	5	6	7	8	9	10
ζ values (mV)	-15.3	-21.3	-24.5	-27.7	-26.9	-28	-29.8
σ	±0.3	±0.2	±1	±0.5	±0.3	±0.8	±1.5

At the start, synthesized particles have a zeta potential value of -29.8 mV at a pH of 10 (Table 3.) Besides, at a pH of 7, ζ-value was -27.7 mV. Therefore, such a high potential value at a pH of 7 indicates that the sericin alone can provide a negative charged electrostatic barrier to nanoparticles. Although no significant change was observed at alkaline conditions, ζ-values were decreased at acidic pHs, from -27.7 to -15.3 mV, approached zero. This situation can be explained by the isoelectronic point of sericin, which is approximately 4 [39].

Agglomeration is a reversible process, which can be defined as the formation of bigger precipitates by weak physical interactions [40]. In this case, agglomeration occurs rather than aggregation because sericin coating acts as a physical barrier even though the protective potential layer was decreased. Therefore, in alkaline pH values, when enough concentration of hydroxyl ion is present in the solution, particles can re-disperse (Figure 4.). These phenomena also could be seen when a complex polymer with electronegativity such as casein [41] is used in nanoparticle synthesis.

pH 4.5 (ζ value= -15.3) is determined as a critical limit for the overwhelming electrostatic forces between particles by attraction forces.

As for the comparison, synthesized NPs have higher surface potential than citrate stabilized nanoparticles (-21.17 mV at pH=7) [42]. Besides, sodium dodecyl sulfate [43] (SDS) and cetyltrimethylammonium bromide [44] (CTAB) coated NPs have the zeta potential of -40 mV and +34 mV, respectively. However, their active stabilization mechanism is only limited by electrostatic repulsion forces due to their amphiphilic structure. Results demonstrate that the Ag-Ser NPs have electrostatic stability between pH range between 5 to 9 with having ζ-value of -27.7 mV at pH=7. Furthermore, Ag-Ser NPs are sterically protected since particles are agglomerated at a pH of 4.5 rather than aggregated.

4. Conclusions

This work successfully integrated silk sericin to Tollens' method for synthesizing silver nanoparticles. Production parameters were optimized by the rate of the synthesis, low-cost ingredients, and non-toxicity of the method. Due to the complex structure and high percentage of hydrophilic groups, sericin molecules provided both electrostatic and steric barriers for nanoparticles. Synthesized Ag-Ser NPs have a narrower average particle size, spherical morphology and show silver's characteristic (111) face-centered cubic

(FCC) plane. Synthesized nanoparticles were agglomerated when the pH of the solution decreased to 4.5, which can be restored to the previous state by increasing pH to higher values, indicating that the steric stabilization between particles continued to act even though electrostatic stabilization was decreased. The proposed approach could potentially synthesize non-toxic, stable silver nanoparticles, thus opening up the way for industrial-scale nanoparticle synthesis.

Associated Content Consist of an image presents silver mirror structure which occur when pH of reaction environment is above 12.

Abbreviations

Ag-Ser NPs: Sericin stabilized silver nanoparticles

FT-IR spectroscopy: Fourier-transforms infrared spectroscopy

DLS: Dynamic light scattering

TEM: Transmission electron microscope

HRTEM: High-resolution transmission electron microscope image

SAED: Selected area (electron) diffraction

Declarations

Associated Content Consist of an image presents silver mirror structure which occur when pH of reaction environment is above 12.

Competing Interests The authors declare that they have no competing interests.

Author Contributions "MS conceptualized the research, conducted the all the experiments, analyzed the experiment data regarding to characterization of nanoparticles and drafted the manuscript. BB helped both the experiments and preparing the manuscript. SM measured particle size of the samples. ST supervised and provided the necessary materials for nanoparticle synthesis. All authors read and approved the final manuscript."

Acknowledgement We would like to thank Dr. Banu Taktak Karaca and Biruni University for valuable contributions including Bradford assay, Zeta-potential measurements. Additionally, our sincere gratitude

to NANOSILVER Kimya Sanayii Ticaret A.Ş. (Chemical Commerce & Industry Co.) for financial support, Dr. Yonca Alkan Göksü for FT-IR measurements and Selçuk University (ILTEK) for TEM images.

References

1. Rao AK, Müller CNR, Cheetham (2006) The Chemistry of Nanomaterials: Synthesis, Properties and Applications. John Wiley & Sons, Inc.
2. Mendes PM (2013) Cellular nanotechnology: Making biological interfaces smarter., " Chem Soc Rev 42(24):9207–9218
3. Tolaymat TM, El Badawy AM, Genaidy A, Scheckel KG, Luxton TP, Suidan M (2010) An evidence-based environmental perspective of manufactured silver nanoparticle in syntheses and applications: A systematic review and critical appraisal of peer-reviewed scientific papers., " Sci Total Environ 408(5):999–1006
4. Eby DM, Schaeublin NM, Farrington KE, Hussain SM, Johnson GR (2009) Lysozyme catalyzes the formation of antimicrobial silver nanoparticles., " ACS Nano 3(4):984–994
5. Mitrano B, Rimmele DM, Wichser E, Erni A, Height R, Nowack (2014) Presence of nanoparticles in wash water from conventional silver and nano-silver textiles., " ACS Nano 8(7):7208–7219
6. Jadhav K (2018) Phytosynthesis of Silver Nanoparticles: Characterization, Biocompatibility Studies, and Anticancer Activity., " ACS Biomater Sci Eng 4(3):892–899
7. Deshmukh SP, Patil SM, Mullani SB, Delekar SD (2019) "Silver nanoparticles as an effective disinfectant: A review," *Mater. Sci. Eng. C*, vol. 97, no. July, pp. 954–965,
8. Maneerung T, Tokura S, Rujiravanit R (2008) Impregnation of silver nanoparticles into bacterial cellulose for antimicrobial wound dressing., " Carbohydr Polym 72(1):43–51
9. Wei L, Lu J, Xu H, Patel A, Chen ZS, Chen G (2015) Silver nanoparticles: Synthesis, properties, and therapeutic applications., " Drug Discov Today 20(5):595–601
10. Zhang XF, Liu ZG, Shen W, Gurunathan S (2016) "Silver nanoparticles: Synthesis, characterization, properties, applications, and therapeutic approaches," *Int. J. Mol. Sci.*, vol. 17, no. 9,
11. Tolaymat TM, El Badawy AM, Genaidy A, Scheckel KG, Luxton TP, Suidan M (2010) "An evidence-based environmental perspective of manufactured silver nanoparticle in syntheses and applications: A systematic review and critical appraisal of peer-reviewed scientific papers," *Science of the Total Environment*, vol. 408, no. 5. Elsevier B.V., pp. 999–1006,
12. Vigneshwaran N, Nachane RP, Balasubramanya RH, Varadarajan PV (2006) A novel one-pot 'green' synthesis of stable silver nanoparticles using soluble starch., " Carbohydr Res 341(12):2012–2018
13. He H (2017) In situ green synthesis and characterization of sericin-silver nanoparticle composite with effective antibacterial activity and good biocompatibility., " Mater Sci Eng C 80:509–516
14. Sivera M et al (2014) "Silver nanoparticles modified by gelatin with extraordinary pH stability and long-term antibacterial activity," *PLoS One*, vol. 9, no. 8,

15. Huang H, Yang X (2004) Synthesis of polysaccharide-stabilized gold and silver nanoparticles: a green method., ” vol. 339:, pp. 2627–2631
16. De Lima CA, Da PS, Silva, Spinelli A (2014) Chitosan-stabilized silver nanoparticles for voltammetric detection of nitrocompounds., ” Sensors Actuators, B Chem 196:39–45
17. Darroudi M, Bin Ahmad M, Abdullah AH, Ibrahim NA (2011) Green synthesis and characterization of gelatin-based and sugar-reduced silver nanoparticles., ” Int J Nanomedicine 6(1):569–574
18. Zain NM, Stapley AGF, Shama G (2014) Green synthesis of silver and copper nanoparticles using ascorbic acid and chitosan for antimicrobial applications., ” Carbohydr Polym 112:195–202
19. Mohan S (2014) Completely green synthesis of dextrose reduced silver nanoparticles, its antimicrobial and sensing properties., ” Carbohydr Polym 106(1):469–474
20. Rocha LKH et al (2017) “Sericin from Bombyx mori cocoons. Part I: Extraction and physicochemical-biological characterization for biopharmaceutical applications,” *Process Biochem.*, vol. 61, no. March, pp. 163–177,
21. Akturk O, Tezcaner A, Bilgili H, Deveci MS, Gecit MR, Keskin D (2011) Evaluation of sericin/collagen membranes as prospective wound dressing biomaterial., ” J Biosci Bioeng 112(3):279–288
22. Yin Y, Li ZY, Zhong Z, Gates B, Xia Y, Venkateswaran S (2002) Synthesis and characterization of stable aqueous dispersions of silver nanoparticles through the Tollens process., ” J Mater Chem 12(3):522–527
23. Kvítek L, Prucek R, Panáček A, Novotný R, Hrbáč J, Zbořil R (2005) The influence of complexing agent concentration on particle size in the process of SERS active silver colloid synthesis., ” J Mater Chem 15(10):1099–1105
24. Aramwit P, Kanokpanont S, Nakpheng T, Srichana T (2010) The effect of sericin from various extraction methods on cell viability and collagen production., ” Int J Mol Sci 11(5):2200–2211
25. Oh H, Young J, Kon M, Chul I, Hoon K (2011) International Journal of Biological Macromolecules Refining hot-water extracted silk sericin by ethanol-induced precipitation., ” Int J Biol Macromol 48(1):32–37
26. Teramoto H, Miyazawa M (2005) Molecular orientation behavior of silk sericin film as revealed by ATR infrared spectroscopy., ” Biomacromolecules 6(4):2049–2057
27. Carolina D, Martínez C, Londoño C, Restrepo-osorio A, Álvarez-lópez C (2017) ScienceDirect ScienceDirect Characterization of sericin obtained from cocoons and silk yarns., ” Procedia Eng 200:377–383
28. Le A (2010) Green synthesis of finely-dispersed highly bactericidal silver nanoparticles via modified Tollens technique., ” Curr Appl Phys 10(3):910–916
29. Panáček A et al (Aug. 2006) “Silver colloid nanoparticles: Synthesis, characterization, and their antibacterial activity,” *J. Phys. Chem. B*, vol. 110, no. 33, pp. 16248–16253,
30. Sangsuk S (2010) Preparation of high surface area silver powder via Tollens process under sonication., ” Mater Lett 64(6):775–777

31. Martínez-Castañón GA, Niño-Martínez N, Martínez-Gutierrez F, Martínez-Mendoza JR, Ruiz F (2008) Synthesis and antibacterial activity of silver nanoparticles with different sizes., ” J Nanoparticle Res 10(8):1343–1348
32. Chen M, Feng YG, Wang X, Li TC, Zhang JY, Qian DJ (May 2007) Silver nanoparticles capped by oleylamine: Formation, growth, and self-organization., ” Langmuir 23(10):5296–5304
33. Philip D (2010) Green synthesis of gold and silver nanoparticles using Hibiscus rosa sinensis., ” Phys E Low-Dimensional Syst Nanostructures 42(5):1417–1424
34. Shankar S, Jaiswal L, Aparna RSL, Prasad RGSV (2014) Synthesis, characterization, in vitro biocompatibility, and antimicrobial activity of gold, silver and gold silver alloy nanoparticles prepared from Lansium domesticum fruit peel extract., ” Mater Lett 137:75–78
35. Guidelli EJ, Ramos AP, Zaniquelli MED, Baffa O (2011) Green synthesis of colloidal silver nanoparticles using natural rubber latex extracted from Hevea brasiliensis., ” Spectrochim Acta - Part A Mol Biomol Spectrosc 82(1):140–145
36. Jyoti K, Baunthiyal M, Singh A (2016) Characterization of silver nanoparticles synthesized using Urtica dioica Linn. leaves and their synergistic effects with antibiotics., ” J Radiat Res Appl Sci 9(3):217–227
37. Levard C, Hotze EM, Lowry GV, Brown GE (2012) Environmental transformations of silver nanoparticles: Impact on stability and toxicity., ” Environ Sci Technol 46(13):6900–6914
38. Vertelov GK, Krutyakov YA, Efremenkova OV, Olenin AY, Lisichkin GV (2008) A versatile synthesis of highly bactericidal Myramistin® stabilized silver nanoparticles., ” Nanotechnology 19:35
39. Wang Z (2014) Exploring natural silk protein sericin for regenerative medicine: An injectable, photoluminescent, cell-adhesive 3D hydrogel., ” Sci Rep 4:1–11
40. Sokolov SV, Tschulik K, Batchelor-McAuley C, Jurkschat K, Compton RG (2015) Reversible or Not? Distinguishing Agglomeration and Aggregation at the Nanoscale., ” Anal Chem 87(19):10033–10039
41. Ashraf S (2013) Colloids and Surfaces B: Biointerfaces Protein-mediated synthesis, pH-induced reversible agglomeration, toxicity and cellular interaction of silver nanoparticles., ” Colloids Surfaces B Biointerfaces 102:511–518
42. Kim I, Lee BT, Kim HA, Kim KW, Kim SD, Hwang YS (Jan. 2016) Citrate coated silver nanoparticles change heavy metal toxicities and bioaccumulation of Daphnia magna., ” Chemosphere 143:99–105
43. Kora AJ, Manjusha R, Arunachalam J (2009) Superior bactericidal activity of SDS capped silver nanoparticles: Synthesis and characterization., ” Mater Sci Eng C 29(7):2104–2109
44. Hedberg J, Lundin M, Lowe T, Blomberg E, Wold S, Wallinder IO (2012) Interactions between surfactants and silver nanoparticles of varying charge., ” J Colloid Interface Sci 369(1):193–201

Figures

Figure 1

FTIR Spectra of freeze dried sericin powder.

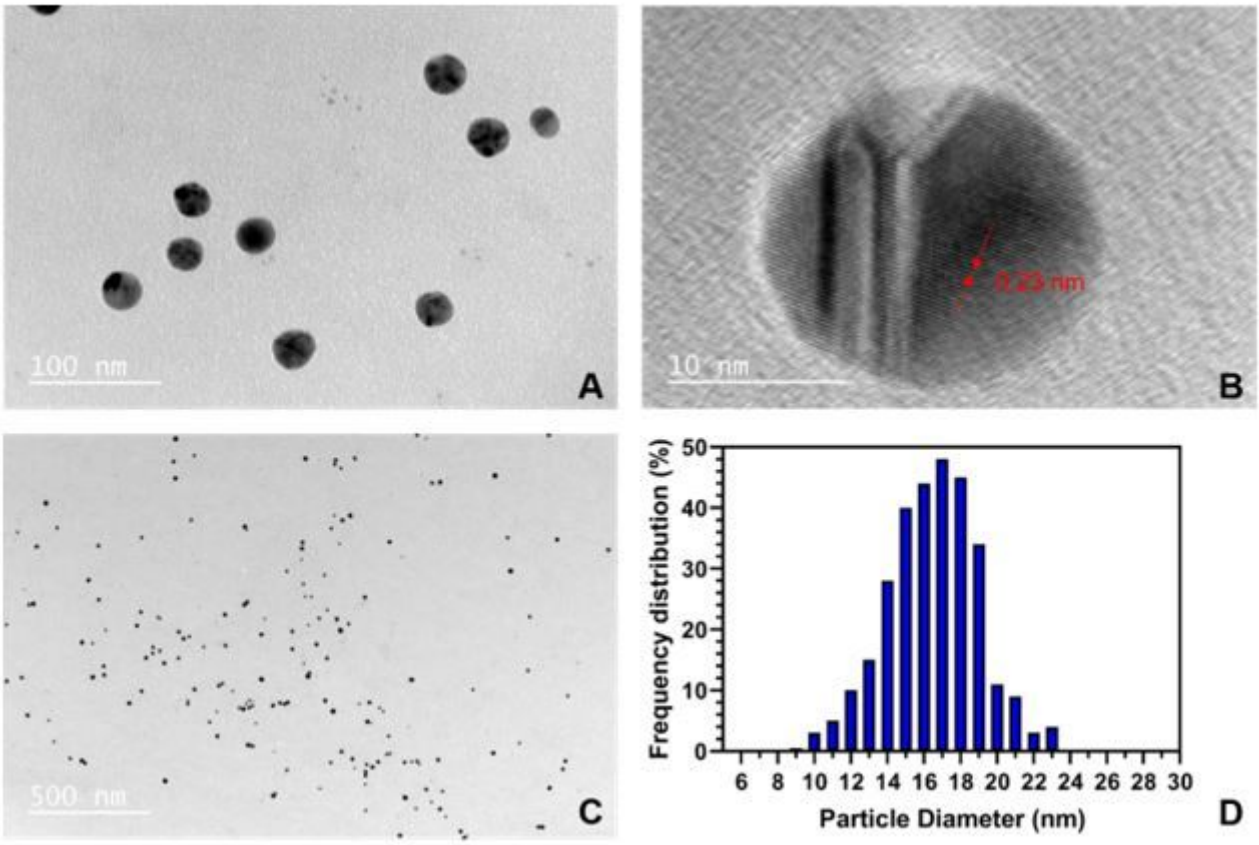

Figure 2

(A) TEM image of synthesized Ag-Ser NPs at 100nm range. (40,000x) (B) HRTEM image of single nanoparticle. (500,000x) (C) 500nm range. (15,000x) (D) corresponding particle size distribution of Figure 3C. (16.03 ± 2.3 nm at 25 µg/mL).

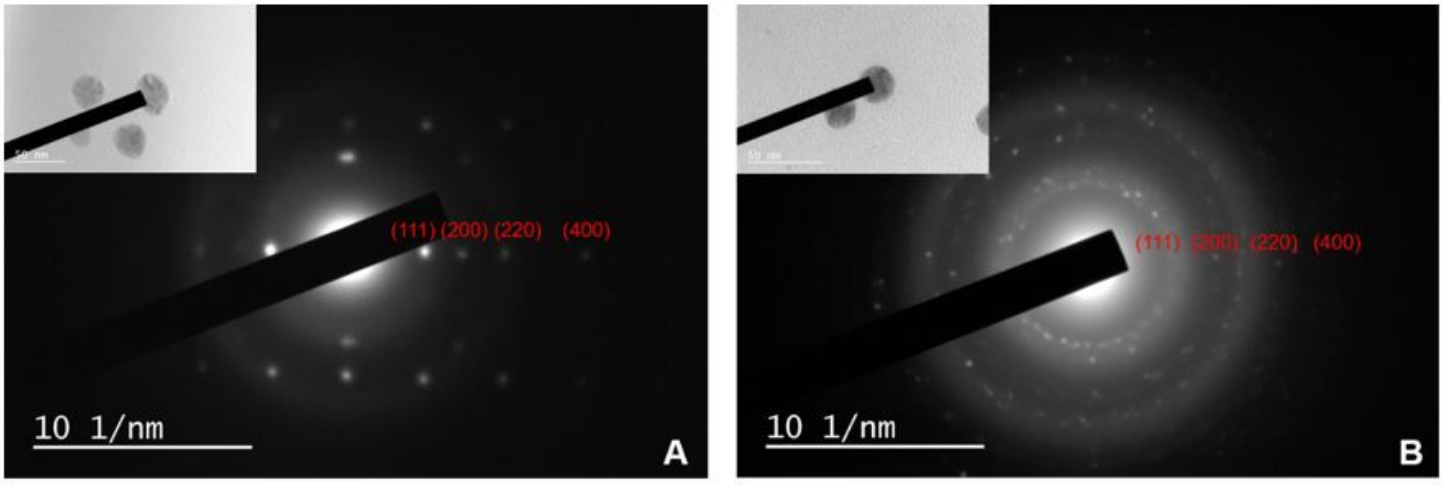

Figure 3

SAED patterns of synthesized Ag-Ser NPs from different particles showing crystallization degree of each individual particle (A-B). The inset of each pattern presents the respective pattern region.

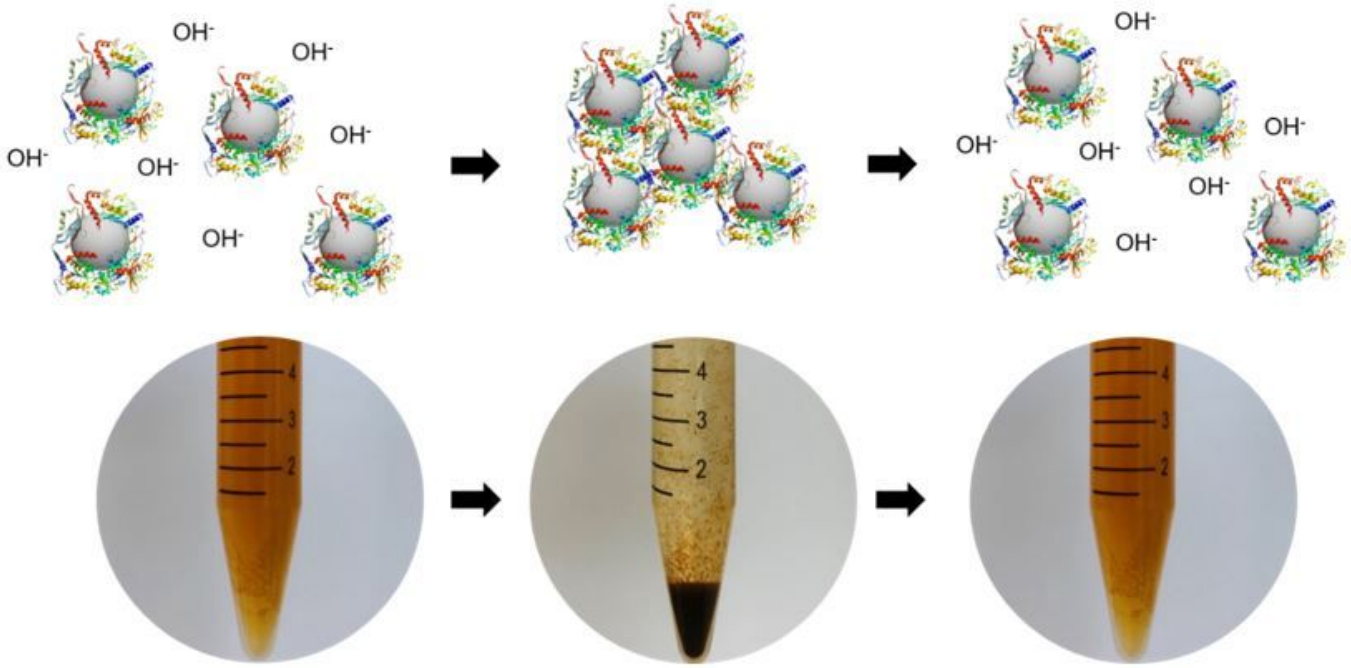

Figure 4

A schematic illustration showing previously agglomerated Ag-Ser NPs at acidic pHs can electrostatically re-stabilize due to protection of steric forces.

Supplementary Files

This is a list of supplementary files associated with this preprint. Click to download.

- SupplementalFile.docx